Available online at www.sciencedirect.com
ScienceDirect
Mathematics and Computers in Simulation 74 (2007) 113–125
MATHEMATICS AND COMPUTERS IN SIMULATION
www.elsevier.com/locate/matcom

A numerical study of the long wave–short wave interaction equations

H. Borluk[a], G.M. Muslu[b], H.A. Erbay[a,*]

[a] *Department of Mathematics, Isik University, Sile Campus, Sile 34980, Istanbul, Turkey*
[b] *Department of Mathematics, Istanbul Technical University, Maslak 34469, Istanbul, Turkey*

Available online 28 November 2006

Abstract

Two numerical methods are presented for the periodic initial-value problem of the long wave–short wave interaction equations describing the interaction between one long longitudinal wave and two short transverse waves propagating in a generalized elastic medium. The first one is the relaxation method, which is implicit with second-order accuracy in both space and time. The second one is the split-step Fourier method, which is of spectral-order accuracy in space. We consider the first-, second- and fourth-order versions of the split-step method, which are first-, second- and fourth-order accurate in time, respectively. The present split-step method profits from the existence of a simple analytical solution for the nonlinear subproblem. We numerically test both the relaxation method and the split-step schemes for a problem concerning the motion of a single solitary wave. We compare the accuracies of the split-step schemes with that of the relaxation method. Assessments of the efficiency of the schemes show that the fourth-order split-step Fourier scheme is the most efficient among the numerical schemes considered.

Keywords: Relaxation method; Split-step method; Long wave–short wave interaction equations; Solitary waves

1. Introduction

The evolution equations describing the interaction between one long longitudinal wave and two short transverse waves propagating in a generalized elastic medium [6] are

$$\mathrm{i}\phi_t + \alpha\phi_{xx} = \beta u\phi, \tag{1.1}$$

$$\mathrm{i}\psi_t + \alpha\psi_{xx} = \beta u\psi, \tag{1.2}$$

$$u_t = \mp\beta(|\phi|^2 + |\psi|^2)_x \tag{1.3}$$

where the real-valued function $u(x,t)$ characterizes the long longitudinal wave and the complex-valued functions $\phi(x,t)$, $\psi(x,t)$ are the slowly varying envelopes of the short transverse waves. The independent variables x and t denote spatial coordinate and time, respectively, and the parameters α and β are real constants. In Eqs. (1.1)–(1.3) the dispersion of the short transverse waves is balanced by the nonlinear interaction of the long longitudinal wave with

* Corresponding author. Tel.: +90 2167121460x2502; fax: +90 2122865796.
E-mail address: erbay@isikun.edu.tr (H.A. Erbay).

0378-4754/$32.00
doi:10.1016/j.matcom.2006.10.016

the short transverse waves, while the evolution of long longitudinal wave is driven by the cumulative effect of the self-interactions of the short-transverse waves. The long wave–short wave interaction (LSI) equations, Eqs., (1.1)–(1.3), have also been derived in [8] for resonant interaction of two short internal waves with a long internal wave in a two-dimensional inviscid incompressible stratified flow. When $\phi \equiv 0$ or $\psi \equiv 0$ or $\phi \equiv p_0\psi$, ($p_0 =$ constant), the LSI equations reduce to the Zakharov–Benney (ZB) equations which have been derived in various fields of physics (see, e.g., [12,1]).

First, we shall briefly mention some of the relevant properties of the LSI equations. Assume that u, ϕ, ψ and all their derivatives converge to zero sufficiently rapidly as $x \to \pm\infty$. Solutions of the LSI equations subjected to these boundary conditions satisfy some conservation laws which imply that the conserved quantities

$$I_0 = \int_{-\infty}^{\infty} u \, \mathrm{d}x, \qquad I_1 = \int_{-\infty}^{\infty} |\phi|^2 \, \mathrm{d}x, \qquad I_2 = \int_{-\infty}^{\infty} |\psi|^2 \, \mathrm{d}x,$$

$$I_3 = \int_{-\infty}^{\infty} \{\mp u^2 + \mathrm{i}(\phi^*\phi_x - \phi\phi_x^*) + \mathrm{i}(\psi^*\psi_x - \psi\psi_x^*)\} \, \mathrm{d}x, \quad I_4 = \int_{-\infty}^{\infty} \{\alpha(|\phi_x|^2 + |\psi_x|^2) + \beta(|\phi|^2 + |\psi|^2)u\} \, \mathrm{d}x \tag{1.4}$$

remain constant in time. The one-soliton solution of the LSI equations, obtained by Ma [8] using the method of inverse scattering, is given by

$$\phi = S(x,t)\cos\,\Theta_0, \qquad \psi = S(x,t)\sin\,\Theta_0, \qquad u = L(x,t) \tag{1.5}$$

where

$$S(x,t) = \left(\mp 2\frac{\alpha}{\beta^2}c\right)^{1/2} \eta \,\mathrm{sech}[\eta(x - ct - x_0)] \exp(\mathrm{i}\Theta(x,t)), \tag{1.6}$$

$$\Theta(x,t) = \frac{c}{2\alpha}x + \left(\alpha\eta^2 - \frac{c^2}{4\alpha}\right)t, \tag{1.7}$$

$$L(x,t) = -2\frac{\alpha}{\beta}\eta^2 \,\mathrm{sech}^2[\eta(x - ct - x_0)]. \tag{1.8}$$

Here η, c, x_0 and Θ_0 are constants. Note that $|\phi|^2 + |\psi|^2 = \pm(c/\beta)u$ for the solution (1.5).

In this study, we propose efficient numerical methods, in particular relaxation and split-step Fourier methods, for solving the LSI equations. In literature there is an emphasis on deriving schemes which conserve discrete analogous of the conserved quantities. Therefore, conservation properties of both the relaxation method and the split-step Fourier method are also discussed. The present relaxation method is based on an extension of the relaxation method introduced in [5] by Besse and Lannes. They have used the relaxation method for solving a two-dimensional generalization of the ZB equations, which describe the propagation of three-dimensional water waves in the case of the long wave–short wave resonance. They have also proved both the existence and uniqueness of a solution of the discrete system and a stability theorem. The convergence of the relaxation method has been proved by Besse [2] for the nonlinear Schrödinger equation. The split-step Fourier method has previously been used for the numerical solution of various nonlinear dispersive wave problems (see, e.g., [7,9–11], and the references therein). For the convergence of the split-step method and error estimates we refer the reader to recent studies by Besse et al. [3,4]. We test the relaxation method and the first-, second- and fourth-order split-step schemes on a problem concerning the motion of a single solitary wave and compare their accuracies and computational costs. These numerical experiments show that both the relaxation method and the split-step Fourier method provide accurate solutions for the LSI equations. Assessments of the efficiency of the schemes show that the fourth-order split-step Fourier scheme is the most efficient among the numerical schemes considered.

The paper is organized as follows. In Section 2, it is shown how the relaxation method and the split-step Fourier method can be reformulated for the LSI equations. In Section 3, the numerical methods are compared from a computational efficiency viewpoint for an initial value problem concerning the motion of a single solitary wave.

2. Numerical methods

2.1. Preliminaries

In this section, we present the relaxation method and the split-step Fourier method for the LSI equations in which use of Fourier series dictates boundary conditions be periodic. For the numerical experiment considered in the next section, the initial conditions of the LSI system are chosen such that ϕ, ψ and u decay to zero sufficiently fast as $|x| \to \infty$. Since application of the numerical method requires truncation of the infinite interval to a finite interval $[a, b]$, the constants a and b are chosen such that the introduction of errors from the boundaries are to be prevented. To simplify the presentation of the Fourier method the spatial period is normalized to $[0, 2\pi]$ using the transformation $X = 2\pi(x - a)/(b - a)$ in which the LSI equations become

$$\mathrm{i}\phi_t + \bar{\alpha}\phi_{XX} = \beta u\phi, \tag{2.1}$$

$$\mathrm{i}\psi_t + \bar{\alpha}\psi_{XX} = \beta u\psi, \tag{2.2}$$

$$u_t = \mp\bar{\beta}(|\phi|^2 + |\psi|^2)_X \tag{2.3}$$

where $\bar{\alpha} = (2\pi/(b-a))^2\alpha$ and $\bar{\beta} = 2\pi\beta/(b-a)$. The interval $[0, 2\pi]$ is then divided into N equal subintervals with grid spacing $\Delta X = 2\pi/N$, where the integer N is even. The spatial grid points are given by $X_j = 2\pi j/N$, $j = 0, 1, 2, \ldots, N$. The time interval $[0, t_\mathrm{F}]$ is divided into M equal subintervals with grid spacing $\Delta t = t_\mathrm{F}/M$. The temporal grid points are given by $t_n = nt_\mathrm{F}/M$, $n = 0, 1, 2, \ldots, M$. The approximate values of $u(X_j, t_n)$, $\phi(X_j, t_n)$ and $\psi(X_j, t_n)$ are denoted by U_j^n, Φ_j^n and Ψ_j^n, respectively.

The discrete Fourier transform of a sequence $\{W_j\}$ for which $j = 0, 1, 2, \ldots, N-1$, i.e.

$$\hat{W}_k = \mathcal{F}_k[W_j] = \frac{1}{N}\sum_{j=0}^{N-1} W_j \exp(-\mathrm{i}kX_j), \quad -\frac{N}{2} \le k \le \frac{N}{2} - 1, \tag{2.4}$$

gives the corresponding Fourier coefficients. Likewise, the sequence $\{W_j\}$ can be recovered from the Fourier coefficients by the inversion formula for the discrete Fourier transform (2.4), as follows:

$$W_j = \mathcal{F}_j^{-1}[\hat{W}_k] = \sum_{k=-\frac{N}{2}}^{\frac{N}{2}-1} \hat{W}_k \exp(\mathrm{i}kX_j), \quad j = 0, 1, 2, \ldots, N-1. \tag{2.5}$$

Here, $\mathcal{F}$ denotes the discrete Fourier transform and $\mathcal{F}^{-1}$ its inverse. These transforms are efficiently computed using a fast Fourier transform (FFT) algorithm. We remark that N must be chosen high enough to avoid aliasing errors and that more sophisticated techniques proposed for controlling aliasing errors will not be considered here.

2.2. Relaxation method

The main idea in the relaxation method is to approximate the first two equations and the last equation of the LSI Eqs. (2.1)–(2.3) in two stages. We treat Eqs. (2.1)–(2.2) and Eq. (2.3) at $t = (n + 1/2)\Delta t$ and $t = n\Delta t$, respectively. Then we use the central difference formula to discretize the derivatives in the LSI equations. We introduce the following relaxation scheme for the LSI Eqs. (2.1)–(2.3):

$$\mathrm{i}\left(\frac{\Phi_j^{n+1} - \Phi_j^n}{\Delta t}\right) + \bar{\alpha}\delta_X^2\left(\frac{\Phi_j^{n+1} + \Phi_j^n}{2}\right) = \beta U_j^{n+1/2}\left(\frac{\Phi_j^{n+1} + \Phi_j^n}{2}\right), \tag{2.6}$$

$$\mathrm{i}\left(\frac{\Psi_j^{n+1} - \Psi_j^n}{\Delta t}\right) + \bar{\alpha}\delta_X^2\left(\frac{\Psi_j^{n+1} + \Psi_j^n}{2}\right) = \beta U_j^{n+1/2}\left(\frac{\Psi_j^{n+1} + \Psi_j^n}{2}\right), \tag{2.7}$$

$$\frac{U_j^{n+1/2} - U_j^{n-1/2}}{\Delta t} = \mp\bar{\beta}\delta_{0X}(|\Phi_j^n|^2 + |\Psi_j^n|^2) \tag{2.8}$$

where we use the difference operators given by

$$\delta_{0X} W_j = \frac{W_{j+1} - W_{j-1}}{2\Delta X}, \qquad \delta_X^2 W_j = \frac{W_{j+1} - 2W_j + W_{j-1}}{(\Delta X)^2} \tag{2.9}$$

for any sequence $\{W_j\}$. We note that Eqs. (2.6) and (2.7) are implicit and a periodic tridiagonal system of equations needs to be solved. However, Eq. (2.8) is explicit and no tridiagonal system needs to be solved. The overall algorithm involves two stages to advance the solution over one time step. First, $U_j^{n+1/2}$ is evaluated explicitly at each of the spatial grid points using Eq. (2.8). Second, Φ_j^{n+1} and Ψ_j^{n+1} are calculated implicitly using Eqs. (2.6) and (2.7), respectively.

The truncation errors for the relaxation scheme are given now. Expanding all the terms of the relaxation scheme (2.6)–(2.8) in Taylor series about the point (X_j, t_n) we obtain the truncation errors T_j^n in the form

$$T_j^n = \left\{ \frac{1}{12}(\Delta t)^2[2\mathrm{i}\phi_{ttt} + 3\bar{\alpha}\phi_{ttXX} - 3\beta(u\phi_{tt} + u_t\phi_t + u_{tt}\phi/2)] + \frac{1}{12}(\Delta X)^2\bar{\alpha}\phi_{XXXX} \right\}_j^n + \mathcal{O}\left((\Delta t)^3 + (\Delta X)^3 + \frac{(\Delta t)^5}{(\Delta X)^2} \right) \tag{2.10}$$

$$T_j^n = \left\{ \frac{1}{12}(\Delta t)^2[2\mathrm{i}\psi_{ttt} + 3\bar{\alpha}\psi_{ttXX} - 3\beta(u\psi_{tt} + u_t\psi_t + u_{tt}\psi/2)] + \frac{1}{12}(\Delta X)^2\bar{\alpha}\psi_{XXXX} \right\}_j^n + \mathcal{O}\left((\Delta t)^3 + (\Delta X)^3 + \frac{(\Delta t)^5}{(\Delta X)^2} \right) \tag{2.11}$$

$$T_j^n = \left\{ \frac{1}{24}(\Delta t)^2 u_{ttt} \pm \frac{1}{6}(\Delta X)^2\beta(\phi_{XXX}\phi^* + 3\phi_{XX}\phi_X^* + 3\phi_X\phi_{XX}^* + \phi\phi_{XXX}^* + \psi_{XXX}\psi^* + 3\psi_{XX}\psi_X^* + 3\psi_X\psi_{XX}^* + \psi\psi_{XXX}^*) \right\}_j^n + \mathcal{O}((\Delta t)^4 + (\Delta X)^4) \tag{2.12}$$

for Eqs. (2.6), (2.7) and (2.8), respectively. We conclude that the relaxation scheme is second-order accurate in both space and time. This is also verified through the numerical experiments presented in Section 3.

We now discuss the conservation properties of the relaxation scheme. In particular, we show that the relaxation scheme conserves the discrete approximations of the conserved quantities I_0, I_1, I_2 and I_4. Note that I_3 is not conserved by the relaxation scheme.

2.2.1. Conservation of I_0 by the relaxation scheme

A discrete approximation of I_0 given by $I_0^{n+1/2} = \Delta X \sum_{j=0}^{N-1} U_j^{n+1/2}$ is conserved in the sense that $I_0^{n+1/2} = I_0^{1/2}$ for all $n \geq 0$. Summing Eq. (2.8) over j we obtain

$$\sum_{j=0}^{N-1} U_j^{n+1/2} = \sum_{j=0}^{N-1} U_j^{n-1/2} \mp \gamma \sum_{j=0}^{N-1} [|\Phi_{j+1}^n|^2 - |\Phi_{j-1}^n|^2 + |\Psi_{j+1}^n|^2 - |\Psi_{j-1}^n|^2]. \tag{2.13}$$

We can easily show that the second term on the right-hand side of this equation is identically zero. Then Eq. (2.13) becomes $I_0^{n+1/2} = I_0^{n-1/2}$ from which we deduce that the relaxation scheme conserves the discrete approximation of I_0.

2.2.2. Conservation of I_1 and I_2 by the relaxation scheme

We now show that a discrete approximation of I_1 given by $I_1^n = \Delta X \sum_{j=0}^{N-1} |\Phi_j^n|^2$ is conserved in the sense that $I_1^n = I_1^0$ for all $n \geq 0$. Multiplying Eq. (2.6) by the $\Phi_j^{*n+1} + \Phi_j^{*n}$ and summing the resulting expression over j we

obtain

$$\frac{\mathrm{i}}{\Delta t}\left[\sum_{j=0}^{N-1}|\Phi_j^{n+1}|^2-\sum_{j=0}^{N-1}|\Phi_j^n|^2\right]+\frac{\mathrm{i}}{\Delta t}\sum_{j=0}^{N-1}(\Phi_j^{n+1}\Phi_j^{*n}-\Phi_j^{*n+1}\Phi_j^n)+\frac{\bar{\alpha}}{2}\sum_{j=0}^{N-1}[(\Phi_j^{*n+1}+\Phi_j^{*n})\delta_X^2(\Phi_j^{n+1}+\Phi_j^n)]$$
$$=\frac{\beta}{2}\sum_{j=0}^{N-1}U_j^{n+1/2}|\Phi_j^{*n+1}+\Phi_j^{*n}|^2. \tag{2.14}$$

Note that the term on the right-hand side of this equation is real. To show that the third-term on the left-hand side of this equation is also real we consider a sequence $\{W_j\}$ $(j=0,1,2,\ldots,N)$ with $W_0=W_N$. Using the identities given by

$$\sum_{j=0}^{N-1}|W_j|^2=\sum_{j=0}^{N-1}|W_{j+1}|^2,\qquad \sum_{j=0}^{N-1}W_j^*W_{j-1}=\sum_{j=0}^{N-1}W_{j+1}^*W_j \tag{2.15}$$

we obtain

$$\sum_{j=0}^{N-1}W_j^*\delta_X^2W_j=\sum_{j=0}^{N-1}|W_{j+1}-W_j|^2$$

which implies that

$$\sum_{j=0}^{N-1}(\Phi_j^{*n+1}+\Phi_j^{*n})\delta_X^2(\Phi_j^{n+1}+\Phi_j^n)=\sum_{j=0}^{N-1}|\Phi_{j+1}^{n+1}-\Phi_j^{n+1}+\Phi_{j+1}^n-\Phi_j^n|^2.$$

Then taking the imaginary part of (2.14) we obtain $I_1^{n+1}=I_1^n$ which shows that the relaxation scheme conserves the discrete approximation of I_1. In a manner completely analogous to that above, one can easily show that the numerical scheme also conserves the discrete approximation of I_2.

2.2.3. Conservation of I_4 by the relaxation scheme

It can be shown that a discrete approximation of I_4 given by

$$I_4^n=\Delta X\sum_{j=0}^{N-1}\left\{\frac{\bar{\alpha}}{(\Delta X)^2}[|\Phi_{j+1}^n-\Phi_j^n|^2+|\Psi_{j+1}^n-\Psi_j^n|^2]+\beta[|\Phi_j^n|^2+|\Psi_j^n|^2]U_j^{n-1/2}\right\} \tag{2.16}$$

is conserved in the sense that $I_4^n=I_4^0$ for all $n\geq 0$. Multiplying Eq. (2.6) by $(\Phi_j^{*n+1}-\Phi_j^{*n})$, summing the resulting expression over j and taking the real part of the resulting equation we obtain

$$\mathrm{Re}\left[\bar{\alpha}\sum_{j=0}^{N-1}(\Phi_j^{*n+1}-\Phi_j^{*n})\delta_X^2(\Phi_j^{n+1}+\Phi_j^n)\right]=\beta\sum_{j=0}^{N-1}U_j^{n+1/2}(|\Phi_j^{n+1}|^2-|\Phi_j^n|^2) \tag{2.17}$$

Using the identities similar to those given in (2.15), after some straightforward calculations we first observe that

$$\mathrm{Re}\left[\sum_{j=0}^{N-1}(\Phi_j^{*n+1}\delta_X^2\Phi_j^n-\Phi_j^{*n}\delta_X^2\Phi_j^{n+1})\right]\equiv 0$$

and then that

$$\mathrm{Re}\left[\sum_{j=0}^{N-1}(\Phi_j^{*n+1}-\Phi_j^{*n})\delta_X^2(\Phi_j^{n+1}+\Phi_j^n)\right]=\frac{-1}{(\Delta X)^2}\sum_{j=0}^{N-1}\left(|\Phi_{j+1}^{n+1}-\Phi_j^{n+1}|^2-|\Phi_{j+1}^n-\Phi_j^n|^2\right). \tag{2.18}$$

Multiplying Eq. (2.8) by $|\Phi_j^n|^2$ and summing the resulting expression over j we obtain

$$\sum_{j=0}^{N-1}(U_j^{n+1/2}-U_j^{n-1/2})|\Phi_j^n|^2 = \mp\bar{\beta}\left(\frac{\Delta t}{2\Delta X}\right)\sum_{j=0}^{N-1}(|\Psi_{j+1}^n|^2-|\Psi_{j-1}^n|^2)|\Phi_j^n|^2,$$

from which we deduce that

$$\sum_{j=0}^{N-1}U_j^{n+1/2}(|\Phi_j^{n+1}|^2-|\Phi_j^n|^2) = \sum_{j=0}^{N-1}\left[U_j^{n+1/2}|\Phi_j^{n+1}|^2-U_j^{n-1/2}|\Phi_j^n|^2 \pm \bar{\beta}\left(\frac{\Delta t}{2\Delta X}\right)(|\Psi_{j+1}^n|^2-|\Psi_{j-1}^n|^2)|\Phi_j^n|^2\right]. \tag{2.19}$$

Using Eqs. (2.18) and (2.19) in Eq. (2.17) we can rewrite Eq. (2.17) in the form

$$-\frac{\bar{\alpha}}{(\Delta X)^2}\sum_{j=0}^{N-1}(|\Phi_{j+1}^{n+1}-\Phi_j^{n+1}|^2-|\Phi_{j+1}^n-\Phi_j^n|^2)$$

$$=\beta\sum_{j=0}^{N-1}\left[U_j^{n+1/2}|\Phi_j^{n+1}|^2-U_j^{n-1/2}|\Phi_j^n|^2 \pm \bar{\beta}\left(\frac{\Delta t}{2\Delta X}\right)(|\Psi_{j+1}^n|^2-|\Psi_{j-1}^n|^2)|\Phi_j^n|^2\right]. \tag{2.20}$$

Following a similar approach for Eq. (2.7) we obtain

$$-\frac{\bar{\alpha}}{(\Delta X)^2}\sum_{j=0}^{N-1}(|\Psi_{j+1}^{n+1}-\Psi_j^{n+1}|^2-|\Psi_{j+1}^n-\Psi_j^n|^2)$$

$$=\beta\sum_{j=0}^{N-1}\left[U_j^{n+1/2}|\Psi_j^{n+1}|^2-U_j^{n-1/2}|\Psi_j^n|^2 \pm \bar{\beta}\left(\frac{\Delta t}{2\Delta X}\right)(|\Phi_{j+1}^n|^2-|\Phi_{j-1}^n|^2)|\Psi_j^n|^2\right]. \tag{2.21}$$

Adding Eqs. (2.20) and (2.21), multiplying the resulting equation by ΔX and noting that

$$\sum_{j=0}^{N-1}[(|\Psi_{j+1}^n|^2-|\Psi_{j-1}^n|^2)|\Phi_j^n|^2+(|\Phi_{j+1}^n|^2-|\Phi_{j-1}^n|^2)|\Psi_j^n|^2]\equiv 0,$$

we obtain $I_4^{n+1}=I_4^n$ which shows that the scheme conserves the discrete approximation of I_4.

2.3. Split-step Fourier method

For the rest of this section, we shall concentrate on the split-step Fourier method for the LSI equations. The basic idea in the split-step method is to decompose the original problem into subproblems which are simpler than the original problem and then to compose the approximate solution of the original problem by using the exact or approximate solutions of the subproblems in a given sequential order. The LSI equations are decomposed into linear and nonlinear subproblems which involve the set of linear uncoupled differential equations

$$\mathrm{i}\phi_t+\bar{\alpha}\phi_{XX}=0, \tag{2.22}$$

$$\mathrm{i}\psi_t+\bar{\alpha}\psi_{XX}=0 \tag{2.23}$$

and the set of nonlinear coupled differential equations

$$\psi_t=-\mathrm{i}\beta u\psi, \tag{2.24}$$

$$\phi_t=-\mathrm{i}\beta u\phi, \tag{2.25}$$

$$u_t=\mp\bar{\beta}(|\phi|^2+|\psi|^2)_X, \tag{2.26}$$

respectively. The novel aspect of the present split-step method lies in the fact that each subproblem is explicitly solvable.

The linear Eqs. (2.22) and (2.23) are solved by means of the discrete Fourier transform and the advancements in time are performed according to

$$\Phi_j^{n+1} = \mathcal{F}_j^{-1}[\exp(-\mathrm{i}\bar{\alpha}k^2\Delta t)\mathcal{F}_k[\Phi_j^n]], \tag{2.27}$$

$$\Psi_j^{n+1} = \mathcal{F}_j^{-1}[\exp(-\mathrm{i}\bar{\alpha}k^2\Delta t)\mathcal{F}_k[\Psi_j^n]]. \tag{2.28}$$

Solutions of the nonlinear subproblem are obtained by assuming

$$\phi = R_1(X,t)\exp[\mathrm{i}\Theta_1(X,t)], \qquad \psi = R_2(X,t)\exp[\mathrm{i}\Theta_2(X,t)] \tag{2.29}$$

where $R_1, R_2, \Theta_1, \Theta_2$ are real-valued functions. Substituting Eq. (2.29) into Eqs. (2.24)–(2.26) and solving the resulting set of differential equations we obtain the analytical solution of the nonlinear subproblem in the form

$$\phi(X,t) = \phi(X,0)\exp\{\mathrm{i}[\pm\tfrac{1}{2}\beta\bar{\beta}t^2(|\phi(X,0)|^2 + |\psi(X,0)|^2)_X - \beta t u(X,0)]\} \tag{2.30}$$

$$\psi(X,t) = \psi(X,0)\exp\{\mathrm{i}[\pm\tfrac{1}{2}\beta\bar{\beta}t^2(|\phi(X,0)|^2 + |\psi(x,0)|^2)_X - \beta t u(X,0)]\} \tag{2.31}$$

$$u(X,t) = \mp\bar{\beta}t(|\phi(X,0)|^2 + |\psi(X,0)|^2)_X + u(X,0). \tag{2.32}$$

The nonlinear terms in Eqs. (2.30)–(2.32) are evaluated in physical space, while the spatial differentiation takes place in spectral space. Then the advancements in time for the nonlinear subproblem are performed by a Fourier pseudospectral method

$$\Phi_j^{n+1} = \Phi_j^n \exp\{\mathrm{i}[\pm\tfrac{1}{2}\beta\bar{\beta}\mathcal{F}_j^{-1}[(\mathrm{i}k)\mathcal{F}_k[(|\Phi_j^n|^2 + |\Psi_j^n|^2)]](\Delta t)^2 - \beta U_j^n\Delta t]\}, \tag{2.33}$$

$$\Psi_j^{n+1} = \Psi_j^n \exp\{\mathrm{i}[\pm\tfrac{1}{2}\beta\bar{\beta}\mathcal{F}_j^{-1}[(ik)\mathcal{F}_k[(|\Phi_j^n|^2 + |\Psi_j^n|^2)]](\Delta t)^2 - \beta U_j^n\Delta t]\}, \tag{2.34}$$

$$U_j^{n+1} = \mp\bar{\beta}\mathcal{F}_j^{-1}[(ik)\mathcal{F}_k[(|\Phi_j^n|^2 + |\Psi_j^n|^2)]]\Delta t + U_j^n. \tag{2.35}$$

An approximation to the solution operator of the LSI Eqs. (2.1)–(2.3) is realized by using a solution operator, that includes an appropriate combination of the solution operators of the linear and nonlinear subproblems. We shall restrict ourselves to the first-, second- and fourth-order split-step schemes for which the splitting formulae are given in [9] (see eqs. (9)–(11) on page 505) and [10] (see eqs. (2.2)–(2.4) on page 584).

We now show for the first-order split-step Fourier scheme that the numerical solution satisfies the discrete conservation laws corresponding to I_0, I_1 and I_2. For this aim we combine the two stages, corresponding to the solutions of linear and nonlinear subproblems, of the first-order split-step scheme in the form

$$\Phi_j^{n+1} = \mathcal{F}_j^{-1}\{\exp(-\mathrm{i}\bar{\alpha}k^2\Delta t)\mathcal{F}_k[P_j^n]\} \tag{2.36}$$

$$\Psi_j^{n+1} = \mathcal{F}_j^{-1}\{\exp(-\mathrm{i}\bar{\alpha}k^2\Delta t)\mathcal{F}_k[Q_j^n]\} \tag{2.37}$$

$$U_j^{n+1} = \mp\bar{\beta}\Delta t\Lambda_j^n + U_j^n \tag{2.38}$$

with the obvious abbreviations

$$P_j^n = \Phi_j^n \exp\{\mathrm{i}[\mp\tfrac{1}{2}\beta\bar{\beta}(\Delta t)^2\Lambda_j^n - \beta\,\Delta t\,U_j^n]\} \tag{2.39}$$

$$Q_j^n = \Psi_j^n \exp\{\mathrm{i}[\mp\tfrac{1}{2}\beta\bar{\beta}(\Delta t)^2\Lambda_j^n - \beta\,\Delta t\,U_j^n]\} \tag{2.40}$$

$$\Lambda_j^n = \mathcal{F}_j^{-1}\{\mathrm{i}k\mathcal{F}_k[|\Phi_j^n|^2 + |\Psi_j^n|^2]\}. \tag{2.41}$$

2.3.1. Conservation of I_0 by the split-step scheme

A discrete approximation of I_0 given by $I_0^n = \Delta X\sum_{j=0}^{N-1} U_j^n$ is conserved in the sense that $I_0^n = I_0^0$ for all $n \geq 0$. Summing Eqs. (2.38) and (2.41) over j we obtain

$$\sum_{j=0}^{N-1} U_j^{n+1} = \mp\bar{\beta}\Delta t\sum_{j=0}^{N-1}\Lambda_j^n + \sum_{j=0}^{N-1} U_j^m \tag{2.42}$$

$$\sum_{j=0}^{N-1} \Lambda_j^n = \sum_{j=0}^{N-1} \sum_{k=-N/2}^{N/2-1} \mathrm{i}k\hat{\Gamma}_k^n \, \mathrm{e}^{\mathrm{i}kX_j} = \sum_{k=-N/2}^{N/2-1} \mathrm{i}k\hat{\Gamma}_k^n \sum_{j=0}^{N-1} \mathrm{e}^{\mathrm{i}kX_j} \tag{2.43}$$

where $\Gamma_j^n = |\Phi_j^n|^2 + |\Psi_j^n|^2$. If we use the orthogonality relation

$$\frac{1}{N}\sum_{j=0}^{N-1} \mathrm{e}^{\mathrm{i}px_j} = \begin{cases} 1, \ p = Nm, \quad m = 0, \mp 1, \mp 2, \ldots \\ 0, \ \text{otherwise} \end{cases}$$

in Eq. (2.43) we obtain $\sum_{j=0}^{N-1} \Lambda_j^m = 0$. Then Eq. (2.42) becomes $I_0^{n+1} = I_0^n$ which shows that the first-order split-step scheme conserves the discrete approximation of I_0.

2.3.2. Conservation of I_1 and I_2 by the split-step scheme

We now show that a discrete approximation of I_1 given by $I_1^n = \Delta X \sum_{j=0}^{N-1} |\Phi_j^n|^2$ is conserved in the sense that $I_1^n = I_1^0$ for all $n \geq 0$. Multiplying eq. (2.36) by the complex conjugate of Φ_j^{n+1} and summing the resulting expression over j we obtain

$$\Delta X \sum_{j=0}^{N-1} |\Phi_j^{n+1}|^2 = \Delta X \sum_{j=0}^{N-1} |\mathcal{F}_j^{-1}\{\exp(-\mathrm{i}\bar{\alpha}k^2\Delta t)\mathcal{F}_k[P_j^n]\}|^2. \tag{2.44}$$

Using the discrete form of Parseval's identity given by

$$\sum_{j=0}^{N-1} |W_j|^2 = N \sum_{k=-N/2}^{N/2-1} |\hat{W}_k|^2,$$

for a sequence $\{W_j\}$ we obtain, after some algebraic manipulations on the right-hand side of (2.44),

$$\begin{aligned} \Delta X \sum_{j=0}^{N-1} |\Phi_j^{n+1}|^2 &= \Delta X \sum_{j=0}^{N-1} \left| \sum_{k=-N/2}^{N/2-1} \hat{P}_k^n \, \mathrm{e}^{-\mathrm{i}\bar{\alpha}k^2\Delta t} \, \mathrm{e}^{\mathrm{i}kX_j} \right|^2 = N\Delta X \sum_{k=-N/2}^{N/2-1} |\hat{P}_k^n \, \mathrm{e}^{-\mathrm{i}\bar{\alpha}k^2\Delta t}|^2 = N\Delta X \sum_{k=-N/2}^{N/2-1} |\hat{P}_k^n|^2 \\ &= \Delta X \sum_{j=0}^{N-1} |P_j^n|^2 = \Delta X \sum_{j=0}^{N-1} |\Phi_j^n|^2 \end{aligned} \tag{2.45}$$

from which we deduce that the first-order split-step scheme conserves the discrete approximation of I_1. Using a similar approach, we can easily show that the numerical scheme also conserves the discrete approximation of I_2.

3. Numerical experiments

To examine the performance of the suggested relaxation and split-step schemes we now consider the problem described below. In the numerical experiments we set $\alpha = \beta = 1$ and take the plus sign in the LSI equations. We remark that the L_2-errors presented below are well correlated with the L_∞-errors. The purpose of the present numerical experiments is to verify numerically (i) that the relaxation scheme exhibits the expected second-order convergence in time while the split-step schemes exhibit the expected first-order, second-order and fourth-order convergence in time, (ii) that the relaxation scheme exhibits the expected second-order convergence in space and (iii) that the fourth-order split-step scheme is computationally more efficient than the others.

If we take $c = 1/2$, $\eta = 1$, $x_0 = 0$ and $\Theta_0 = \pi/4$ in Eqs. (1.6) and (1.5), the initial condition corresponding to the solitary wave solution (1.5) becomes

$$\phi(x,0) = \psi(x,0) = \frac{1}{\sqrt{2}}\mathrm{sech}(x)\exp\left(\frac{\mathrm{i}x}{4}\right), \qquad u(x,0) = -2\mathrm{sech}^2 x. \tag{3.1}$$

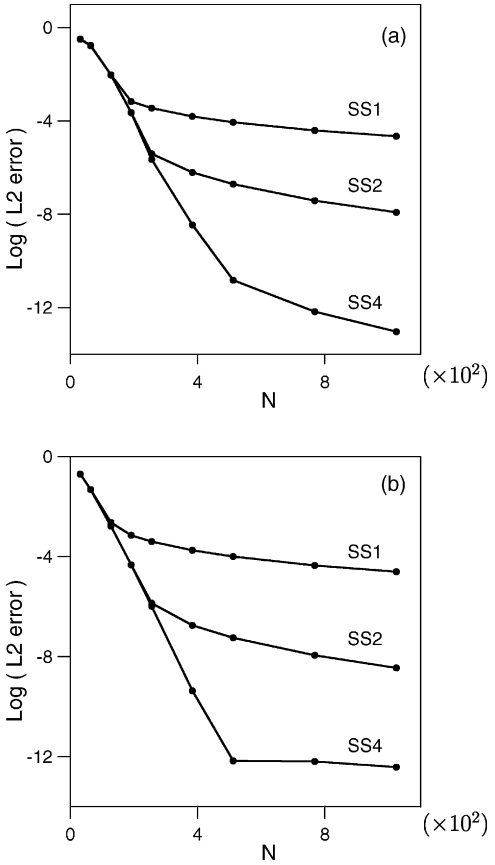

Fig. 1. The L_2-errors at the terminating time $t_F = 1$ as a function of the number of spatial grid points for the first-order (SS1), second-order (SS2) and fourth-order (SS4) split-step Fourier schemes. (a)The L_2-error for u, (b) the L_2-error for ϕ.

We advance the solution to final time $t_F = 1$. To balance the error due to the boundary effects with the error due to internal resolution, an optimal space interval is chosen and the problem is solved on $-40 \leq x \leq 40$. It follows from (1.4) that the exact values of the conserved quantities are $I_0 = -4$, $I_1 = 1$, $I_2 = 1$, $I_3 = 4.3\bar{3}$, $I_4 = -1.875$.

We present in Fig. 1(a and b) the L_2-errors related to the unknowns u and ϕ, respectively, for the first-order (SS1), second-order (SS2) and fourth-order (SS4) split-step schemes for the final time $t_F = 1$ as a function of N. We choose the value of Δt for a given Δx ($\equiv (b-a)/N$) so that $\Delta t = \nu(\Delta x)^2$, where the value of ν is fixed at $\nu = 0.0277$. As expected, the notable outcome of this figure is the higher accuracy of the fourth-order split-step Fourier method. As the order of the split-step scheme increases, the number of grid points must be decreased to maintain the same error. We present in Fig. 2 the L_2-errors related to u and ϕ for the relaxation scheme at the final time $t_F = 1$ as a function of N in which the value of Δt for a given N is chosen so that $\Delta t = \Delta x$. A comparison with the split-step schemes shows that the split step schemes can produce accurate results on a reasonably coarse mesh. The fourth-order split-step scheme is seen to have accuracy properties superior to the relaxation scheme.

To test whether the proposed numerical schemes exhibit the expected convergence rates in time we perform some numerical experiments for various values of Δt and a fixed value of N. In these experiments we take $N = 1024$ and $N = 10^5$ for the split-step schemes and the relaxation scheme, respectively, to ensure that the spatial error is negligible. The rate of convergence for each scheme is calculated using the formula

$$\text{rate of convergence} \approx \frac{\ln(E(N_2)/E(N_1))}{\ln(N_1/N_2)} \tag{3.2}$$

where $E(N_j)$ is the L_2-error when using N_j subintervals. The L_2-errors for the terminating time $t_F = 1$ and the corresponding convergence rates are shown in Tables 1–3. Because we have eliminated the spatial discretization

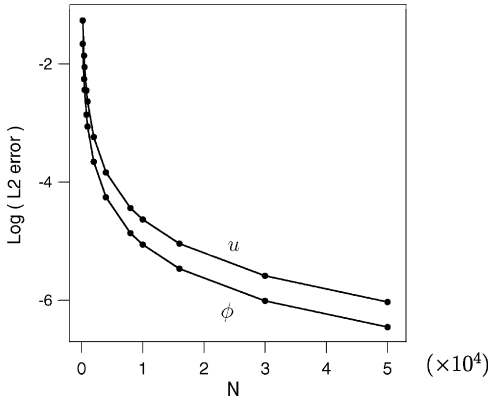

Fig. 2. The L_2-errors for u and ϕ at the terminating time $t_F = 1$ as a function of the number of spatial grid points for the relaxation scheme.

Table 1
Comparison of the convergence rates in time calculated from the L_2-errors of u for the first-order, second-order and fourth-order split-step Fourier schemes ($N = 1024$)

Δt	SS1		SS2		SS4	
	L_2-error (u)	Order	L_2-error (u)	Order	L_2-error (u)	Order
0.0200	2.709E−3	–	1.702E−4	–	1.034E−5	–
0.0100	1.324E−3	1.032	4.253E−5	2.000	6.835E−7	3.919
0.0050	6.545E−4	1.016	1.063E−5	2.000	4.335E−8	3.978
0.0020	2.600E−4	1.007	1.701E−6	1.999	1.114E−9	3.995
0.0010	1.297E−4	1.003	4.252E−7	2.000	6.970E−11	3.998
0.0005	6.478E−5	1.001	1.063E−7	2.000	4.357E−12	3.999

Table 2
Comparison of the convergence rates in time calculated from the L_2-errors of ϕ for the first-order, second-order and fourth-order split-step Fourier schemes ($N = 1024$)

Δt	SS1		SS2		SS4	
	L_2-error (ϕ)	Order	L_2-error (ϕ)	Order	L_2-error (ϕ)	Order
0.0200	2.949E−3	–	4.901E−5	–	4.535E−7	–
0.0100	1.473E−3	1.001	1.225E−5	2.000	2.890E−8	3.971
0.0050	7.362E−4	1.000	3.063E−6	1.999	1.815E−9	3.993
0.0020	2.943E−4	1.000	4.901E−7	1.999	4.655E−11	3.997
0.0010	1.471E−4	1.000	1.225E−7	2.000	2.911E−12	3.999
0.0005	7.358E−5	0.999	3.063E−8	1.999	2.204E−13	3.723

errors, the errors on the tables are due to time discretizations solely. The computed convergence rates agree well with the expected rates for both the relaxation scheme and the split-step schemes. As it is expected from the truncation errors given in Section 2, the relaxation scheme is of the same order in Δt as the second-order split-step scheme.

To test whether the relaxation scheme exhibits the expected convergence rate in space we perform some further numerical experiments for various values of N and a fixed value of Δt. In these experiments, we take $\Delta t = 10^{-4}$ to minimize temporal errors. The results are shown in Table 4 for an increasing number of subintervals. We present the

Table 3
The convergence rates in time calculated from the L_2-errors of u and ϕ for the relaxation method ($N = 100000$)

Δt	L_2-error (u)	Order	L_2-error (ϕ)	Order
0.040	1.436E−4	–	1.193E−4	–
0.020	3.590E−5	2.000	2.983E−5	1.999
0.010	8.877E−6	2.015	7.451E−6	2.001
0.005	2.116E−6	2.068	1.856E−6	2.005

Table 4
The convergence rate in space for the relaxation method ($\Delta t = 10^{-4}$)

N	L_2-error (u)	Order	L_2-error (ϕ)	Order
1, 000	2.629E−3	–	8.069E−4	–
2, 500	4.208E−4	1.999	1.289E−4	2.001
5, 000	1.052E−4	2.000	3.223E−5	1.999
10, 000	2.630E−5	2.000	8.058E−6	1.999
20, 000	6.575E−6	2.000	2.014E−6	2.000

L_2-errors for the terminating time $t_F = 1$ together with the observed rates of convergence in each case. While the split-step schemes are of spectral-order accuracy, these results show that the relaxation scheme is only second-order accurate in space.

The conservation properties of the numerical schemes are examined by investigating the variations of the discrete approximations of the conserved quantities with time. To obtain a better visualization we depict the variations of the conservation errors $e_k(t) = \bar{I}_k - \bar{I}_{k0}$, $(k = 0, 1, 2, 3, 4)$, where $\bar{I}_k$ and $\bar{I}_{k0}$ represent the calculated value of the conserved quantity I_k at time t and $t = 0$, respectively. We present in Fig. 3 the conservation errors e_k as functions of time for the relaxation method with $N = 10^3$ and $\Delta t = 2 \times 10^{-4}$. It is evident that there is no hint of any variation in the magnitudes of e_0, e_1, e_2 and e_4. In fact the variations in the magnitudes of these conservation errors are less than 10^{-12} and therefore there are no visible differences in their graphical results. However, the time evolution of e_3 is quite different from those of e_0, e_1, e_2 and e_4 and the magnitude of e_3 increases as time increases. These numerical results allow us to conclude that the conserved quantities I_0, I_1, I_2 and I_4 are extremely well preserved for the relaxation method while the conserved quantity I_3 is not preserved. In addition, we remark that these are consistent with the analytical results obtained in Section 2.2. We perform a similar investigation for all of the split-step schemes presented here with $N = 1024$, $\Delta t = 0.169491 \times 10^{-3}$. The corresponding figures will not be presented here due to space limitations. We observe that the variations in the magnitudes of the conservation errors e_0, e_1, e_2 are always less than 10^{-11}. This implies that the conserved quantities I_0, I_1 and I_2 are extremely well preserved for the split-step schemes. This is consistent with the analytical results obtained in Section 2.3.

In Fig. 4(a and b), we plot the L_2-errors for u and ϕ, respectively, versus the amount of computing time needed by each scheme to achieve those errors. A horizontal line through a particular value of the error intersects the graphs at the CPU time needed by each scheme. The most efficient scheme is the one that uses the least CPU time to produce a solution of given accuracy. In fact, the CPU times cannot be compared directly since the numerical schemes have not been optimized, but the figure may give an indication of the efficiency of the present methods. We observe from Fig. 4 that the fourth-order scheme is more efficient than the second-order scheme when considering an error of less

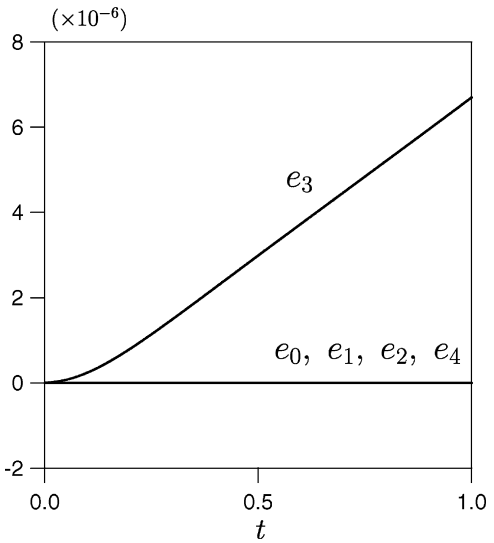

Fig. 3. The conservation errors e_k $(k = 0, 1, 2, 3, 4)$ as functions of time for the relaxation scheme ($N = 10^3$, $\Delta t = 2 \times 10^{-4}$).

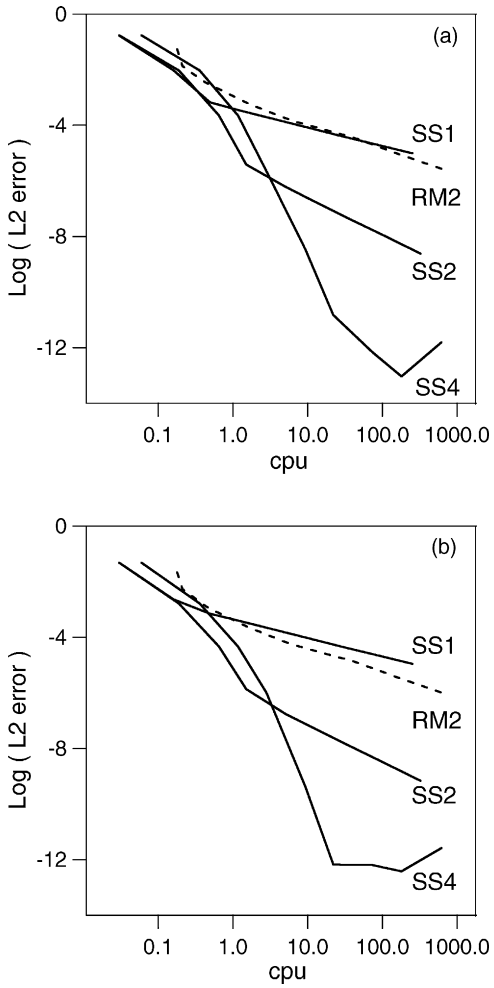

Fig. 4. The L_2-errors for the terminating time $t_F = 1$ as a function of the CPU time for the relaxation method (RM2) and the first-order (SS1), second-order (SS2) and fourth-order (SS4) split-step Fourier schemes. (a)The L_2-error for u, (b) the L_2-error for ϕ.

than 10^{-6}. The difference in computational efficiency becomes more significant as the accuracy level is increased. A similar situation is observed for the L_2-error levels less than roughly 10^{-3} when comparing the second-order split-step scheme with both the first-order split-step scheme and the relaxation scheme. We conclude that the fourth-order split-step scheme is computationally more efficient than the remaining numerical schemes, particularly when high accuracy is required.

Acknowledgements

The authors are grateful to Professor S. Erbay for many useful discussions. The authors also thank the anonymous referees for insightful comments.

References

[1] D.J. Benney, A general theory for interactions between short and long waves, Stud. Appl. Math. 56 (1977) 81–94.
[2] C. Besse, A relaxation scheme for nonlinear Schrödinger equation, SIAM J. Numer. Anal. 42 (2004) 934–952.
[3] C. Besse, B. Bidegaray, S. Descombes, Order estimates in time of splitting methods for the nonlinear Schrödinger equation, SIAM J. Numer. Anal. 40 (2002) 26–40.

[4] C. Besse, N. Mauser, H.-P. Stimming, Numerical study of the Davey-Stewartson system, M2AN Math. Modell. Numer. Anal. 38 (2004) 1035–1054.
[5] C. Besse, D. Lannes, A numerical study of the long-wave short-wave resonance for 3D water waves, Eur. J. Mech. B-Fluids 20 (2001) 627–650.
[6] S. Erbay, Nonlinear interaction between long and short waves in a generalized elastic solid, Chaos Soliton Fract. 11 (2000) 1789–1798.
[7] B. Fornberg, T.A. Driscoll, A fast spectral algorithm for nonlinear wave equations with linear dispersion, J. Comput. Phys. 155 (1999) 456–467.
[8] Y.C. Ma, The resonant interaction among long and short waves, Wave Motion 3 (1981) 257–267.
[9] G.M. Muslu, H.A. Erbay, A split-step Fourier method for the complex modified Korteweg-de Vries equation, Comput. Math. Appl. 45 (2003) 503–514.
[10] G.M. Muslu, H.A. Erbay, Higher-order split-step Fourier scehemes for the generalized nonlinear Schrödinger equation, Math. Comput. Simulat. 67 (2005) 581–595.
[11] S. Yu, S. Zhao, G.W. Wei, Local spectral time splitting method for first- and second-order partial differential equations, J. Comput. Phys. 206 (2005) 727–780.
[12] V.E. Zakharov, Collapse of Langmuir waves, Sov. Phys. JETP 35 (1972) 908–914.